Deriving urban neighborhood characteristics using spatial autocorrelation measures

DeepthiDurgi, Mark Brussel*, DevidasTambe, Alfred Stein, Mark Zuidgeest and Martin van Maarseveen

Abstract

This paper addresses the detection and characterization of urban neighborhoods from remote sensing images. Object based image analysis (OBIA) procedure is implemented and spatial statistical methods are applied to create homogeneous zones. Both Getis-Ord statistic and shape metrics are used. These methods are applied to the data of Pune city, India. Five types of neighborhoods were identified, all clearly dissimilar from each other. Such understanding of the neighborhood structure from data is considered well-suited, in non-motorized transportation (NMT) planning studies. Also, neighborhood scale is a fairly neglected level in transportation planning, and this research suggests a method to extract rational neighborhoods for such simulations. The study closes, demonstrating a promising and consistently applicable procedure to provide an urban neighborhood structure from remote sensing images. Validation is done using travel data from a trip survey. The study calls for further research to develop transport models from the neighborhood scale.

Keywords: Urban neighborhood, OBIA, Getis-Ord, Non-motorized transportation (NMT).

M.J.G. Brussel (Corresponding author)
Department of Urban and Regional Planning and Geoinformation Management, Faculty ITC, University of Twente, the Netherlands
Email: m.j.g.brussel@utwente.nl

1. Introduction

Cities are complex spatial systems, composed of physical elements like buildings, vegetation, vacant lands, water bodies, and roads. With diversities in urban form, spatial interaction occurs at different scales. Physical elements of cities can be grouped by homogeneity, into blocks, sports parks and residential districts. In this paper, we attempt to define homogenous zones as "neighborhoods", which are essential to non-motorized transport planning analysis and applications. One could consider neighborhoods as a conglomerate of physical elements of different types and as units, they help planners understand urban form, which is essential to estimate travel demand.

We characterize a neighborhood by its relative homogeneity, described by the measures, density, texture, pattern and clustering, applied on the physical elements. The following sections provide references to the literature, accommodating the "neighborhood" characterization in this research. In urban studies, neighborhoods constitute a fundamental unit of interest for many researchers. Indeed, neighborhoods are considered as genuine phenomena, as illustrated by the Chicago School (Park and Burgess, 1921; Shaw and McKay, 1942). Psychologists have focused on the effect of neighborhood contexts on individual-level processes (Bronfenbrenner, 1977). Multi-level modeling tools have been used to consider the effects of neighborhood characteristics on delinquent behavior (Osgood and Anderson, 2004; Silver and Miller, 2004), educational achievement (Ainsworth, 2002), low birth weight (Morenoff, 2003), depression (Ross et al., 2000) and satisfaction (Hipp, 2010). Cao et al. (2009) show how residential location choices in a city depend upon the neighborhood characteristics. Schwanen and Mokhtarian (2005) study the relationship between neighborhood structure of home locations and the travel distance. These studies discretely conceptualize what constitutes a neighborhood. Census-blocks, block groups, postal zip code blocks and neighborhoods, defined by residents themselves, all form neighborhoods in many studies. Nevertheless, most studies face a common challenge, i.e. how to illustrate neighborhoods as rational units. Traffic Analysis Zones (TAZs) in transport studies generally are huge areas. The much needed neighborhood scale is a neglected level, in such analysis. This is problematic, particularly with regard to non-motorized transport (NMT) trips (walking and cycling) that tend to have shorter distances.

We derive urban neighborhoods from remote sensing images, based on the extraction and classification of built-up area objects and their pattern analysis. Quick Bird imagery with a spatial resolution of 0.6 m proves advantageous in detecting the homogeneity in built environment. Recently, object based image analysis (OBIA) methods have been developed, proving their potential in providing accurate urban classification results (Ebert et al., 2009; Sliuzas et al., 2008). Applying spatial autocorrelation measures, Jupp et al.(1988) show that interrelationships between size, shape and density of the objects determine the spatial structure. We chose spatial autocorrelation measures, to characterize neighborhoods centered on the building footprints.

We apply OBIA to derive built up areas (objects) from the imagery. We then, combine the objects, with spatial prediction by Kriging, to detect homogeneity and to smooth the otherwise heterogeneous patches. Variogram analysis is applied at this point, to interpret the pattern of built up areas. Further, Getis-Ord∗ statistic is used to understand the clustering of built up areas obtained from OBIA. Subsequently, we are able to classify the clusters obtained, into five kinds of "neighborhoods". Spatial metrics relating to the built up objects in each of the neighborhoods, explain the variation and significance of the typology, aiding us in interpreting the neighborhood model results.

Section 2 discusses the methods used in the study. Under section 3, we discuss and interpret the key outputs and illustrate the neighborhoods extracted. We attempt to corroborate the neighborhoods, with the help of NMT travel data (Bicycle Volumes) and find a clear distinction in the volumes recorded per neighborhood type. The results give a stimulus to the assumption this research makes ie., homogeneity in built up areas impacts the travel behavior, in the context of NMT modes, in Indian context. Under section 4, we reflect on the methods applied, the outcome and close with our submissions for further research.

2. Materials and Methods

2.1 Location and data

Pune city, in India is an administrative capital with 5.5 million inhabitants. Situated 560 m above sea level the oldest part of the city, originating from the 5th century, is called Central Pune. Since 1970s, Pune has seen a

rapid growth in population and area. Suburban areas have been annexed to the city and it grew outward.

The Quick Bird image we use, comprises the red (630-690 nm), green (520-600 nm) and blue (450-520nm) bands. A subset of size 2.56 by 1.78 km is selected, with geographic locations, 18° 29' 53.5" N to 18° 31' 16.7" N and 73° 50' 2.8" E to 73° 51' 2.9" E (Fig. 1), in central Pune.

Fig.1: A subset of pan-sharpened Quick Bird image(Size= 1.78 by 2.56 km)

2.2. Defining Urban form through" Neighborhoods"

Central to this study is the understanding we bring to urban form, through "Neighborhoods". Urban form is defined by the spatial configuration of fixed elements in cities (Anderson, Kanaroglou, and Miller, 1995). According to Schwarz (2010), it can be quantified using indicators in two broad categories i.e. landscape metrics or form based indicators and socio-economic indicators. The former, relies on the indicators, obtained from im-

agery or survey data. The latter, is usually obtained through spatial constructs like census tracts, wards, TAZs (Kwan and Weber 2008). Song and-Knaap (2007), identify relevant attributes of physical urban form to compute a limited set of indicators.

To map neighborhoods, homogenous urban objects have to be grouped and analyzed, using composite variables (Stead and Marshall, 2001). Clustering these variables can then reveal urban form, resulting in identifying neighborhood types (Yoshida and Omae, 2005; Song and Knaap, 2007). Spatial clustering depends upon the conjecture that there is spatial autocorrelation among nearby values (Getis, 2010). Thus, we understand that neighborhoods are characterized by a set of variables, such as the density of buildings, lengths and category of roads, extent of green spaces and water bodies.

A large body of empirical evidence supports the method of validating neighborhoods against travel data, on the foundation that urban form influences travel behavior. Trip lengths, volume and mode can be used to represent travel behavior (Frank and Pivo, 1994; Cervero and Kockelman, 1997; Stead and Marshall, 2001; Ewing and Cervero, 2010; Gim, 2012). Therefore, we use travel data to validate the neighborhood typology obtained. (Note: Bicycle volume data from a travel behavior survey in Pune has been used).

2.3 Segmentation and statistical components

OBIA is applied to classify urban land cover classes from building footprints (BFP) using spectral and contextual information. Six land cover classes were distinguished, i.e. vegetation, shadow, water body, bare soil, road, built-up area. To derive the BFP feature dataset, OBIA with multi-resolution segmentation was employed (Table 1). BFPs however, are only partly visible in QuickBird images. Therefore they were generated by combining partial footprints with building rooftops that are detected easily. An OBIA ruleset was defined, summarizing the segmentation. Utilizing spectral information, a value of 0.1 for the shape parameter was selected for segmentation, whereas equal weights (0.5) were given to smoothness and compactness. Heterogeneity between objects was quantified by the scale parameter. Its value affects image segmentation, determining the size of image objects. A high scale value corresponds to image objects that are relatively large and hence to high variability within each object and vice versa. By a coherent trial-and-error procedure, the scale parameter was set to 20, a value corresponding to 12m. This value segments the areas well, as the minimum size

of the buildings in Pune city correspond to it. The OBIA rule-set, that defines the class hierarchy, is presented below. By omission strategy, this rule-set excludes non-built up objects. As suggested by Chen et al. (2007), we generate a rule-set of three levels. Level one delineates bare soil; level two differentiates between water, vegetation and non-vegetation; level three subdivides non- vegetated land, i.e. urban built-up areas, into BFPs and other urban objects. Definitions of training samples using color composites as suggested by Tang et al. (2008) were used to classify the objects. Conditional information from the three levels, contextual information from the scale parameter and attribute information provided by the reflectance values, together, define each class.

Land cover class	Description
Vegetation	*NRB*> 0.05
Shadow	Brightness < 225 and $1/3(\sigma_r+\sigma_g+\sigma_b) < 10$
Water body	Mean *b*< 285 and $1/3(\sigma_r+\sigma_g+\sigma_b) < 7$ and *NRB*> 0.05 and $\sigma_b < 6$
Open space	*b*< 320 and Classified building footprint area > 1450 sq m
Road	Length/width ration > 3.5 and $\sigma_b < 12$
Building footprints	Brightness > 420

Table 1: OBIA rule set definitions for image classification. NIR = Near Infrared, and σr,σb,σg are the standard deviations for the red, blue and green band, respectively.

To classify image objects, class definitions were generated for each land cover type, applying the Normalized Red Blue (NRB) ratio, based on the blue and red spectral bands:

$$NRB = \frac{\mu B - \mu R}{\mu B + \mu R} \quad (1)$$

Where μB is the mean DN object value in the blue spectral band and μR is the mean DN object value in the red spectral band

2.4. The Getis–Ord(G_i^*) local spatial statistic

Similar urban types show clustering in DN reflectance on spectral bands. Similar clusters can be observed, if we consider their spatial location. Here, we analyze the spatial pattern of built-up area. Getis–Ord(G_i^*) local spatial statistic serves the purpose (Getis 2010). It quantifies the degree of clustering of BFPs with either high values or low values.

Let there be n BFPs, and let yj be the area of BFP j with its average $\overline{y}$ and standard deviation s. Further, let uij, be the weight for pixel (i,j), i.e. the inverse Euclidean distance between BFPs I and j raised to the power α (α ≥ 1): $u_{ij} = d_{ij}^{-\alpha}$ with $\alpha \geq 1$. As a consequence,$\sum_{j=1}^{n} u_{ij}(d)y_j$ is the sum of the areas within distance d of BFP i, including footprint I itself. Let u_i^*be the number of the BFPs within d of BFP i, i.e. $u_i^* = u_i + u_{ii}$.

Then the Getis-Ord statistic is defined as

$$G_i^*(d) = \frac{\sum_{j=1}^{n} u_{ij}(d)y_j - u_i^*\overline{y}}{s\{[(ns_{1i}^*) - u_i^{*2}]/(n-1)\}^{\frac{1}{2}}} \text{ for all } i \quad (2)$$

where

$s_{1i}^* = \sum_{j=1}^{n} u_{ij}^2$.

The search threshold distance d and the power α determine the role of the ith observation. We set α = 1 initially and d equals 112.5 m. This ensured that each building had at least one neighboring building. Centroids and area of the BFPs were used as the location and associated values.

G_i^*measures the deviation of a local pattern, from the average value of the attribute (Lin 2004).It can take both positive and negative values to individual footprints. Following LeDrew, et al (2004), a dense cluster of BFPs results in a positive G_i^* value, whereas a sparse patch shows a negativeG_i^* value, and a value close to 0 indicates a random distribution of BFPs. As the

limiting case, G_i^* follows the normal distribution which can then be used for testing whether it is significantly different from 0.

2.5. Spatial interpolation

We use ordinary Kriging to generate contours for clustering. Kriging is based upon the variogram and measures the spatial variation as a function of distance between locations (Gómez-Hernández, 2005; Curran and Atkinson, 1998). In the absence of a trend, the variogram is defined as depending only on the separation vector h (Atkinson 2002) as:

$$\gamma(h_{i,i+h}) = \frac{1}{2}E[\{G_i^*(d) - G_{i+h}^*(d)\}^2] \quad (3)$$

By replacing the expectation by squared pair differences of the observations the empirical variogram is obtained where the pairs are grouped into distance classes. Through the empirical variogram, the parameters of a permissible variogram model are fitted. We use a spherical model similar to the study by Isaaks et al. (1989)

$$\gamma(h) = \begin{cases} 0 \text{ for } h = 0 \\ c_0 + c_1\left(1.5\frac{h}{a} - 0.5\left(\frac{h}{a}\right)^3\right) \text{ for } 0 < h < a \\ c_0 + c_1 \text{ for } a \le h \end{cases} \quad (4)$$

With parameters c0 (the nugget variance), c1 (the partial sill), and a(the range). Using the variogram, ordinary Kriging predicts values at unvisited locations as the weighted sum of observations:

$$G_0^* = \sum_{i=1}^{n} w_i G_i^* \quad (5)$$

where, G_0^* is the predicted value at the un-sampled location, wi are weights that have to minimize the variance of Kriging prediction error, and the G_i^* are values at the sampled locations. weights wi are obtained from the ordinary Kriging system:

$$\gamma_{i0} = \sum_{j=1}^{n} w_j \gamma_{ij} + \mu \quad for\ all\ i = 1, \dots, n \quad (6)$$

where, γij are variogram values for the distances between observation locations I and j and γi0 are the variogram values for the distances between the i[th]observation and the prediction location. μis a Lagrange multiplier.

From equation (6), solution for the weights is as follows (Gómez-Hernández 2005):

$$\begin{bmatrix} w_{10} \\ w_{20} \\ . \\ . \\ w_{n0} \\ \mu \end{bmatrix} = \begin{bmatrix} \gamma_{11} & \gamma_{12} & \cdot\cdot & \gamma_{1n} & 1 \\ \gamma_{21} & \gamma_{22} & \cdot\cdot & \gamma_{2n} & 1 \\ . & . & \cdot\cdot & . & . \\ . & . & \cdot\cdot & . & . \\ \gamma_{n1} & \gamma_{n2} & \cdot\cdot & \gamma_{nn} & 1 \\ 1 & 1 & \cdot\cdot & 1 & 0 \end{bmatrix}^{-1} \cdot \begin{bmatrix} \gamma_{10} \\ \gamma_{20} \\ . \\ . \\ \gamma_{n0} \\ 1 \end{bmatrix}. \quad (7)$$

We create the neighborhood map using average Z-score values. Threshold contour Ct was derived to determine their boundaries. Selection of Ct was done by applying selected contours CDN of several DN values. We select brightness and blue band digital numbers between 260 and 320 with an interval of 5. Average G_i^* value was calculated for the obtained polygons for several CDNst. Final neighborhood contour Ct, best reveals the neighborhood boundaries, showing homogeneity. Neighborhoods thus obtained were then interpreted and grouped into neighborhood types. We obtain an integrated map, showing neighborhood type, expanding the method used on the subset, on the remaining datasets.

2.6. Neighborhood type and characterization

Characterizing neighborhood types is an essential final step for interpreting the results obtained. For this purpose, spatial metrics are chosen. Spatial metrics are measurements derived from digital analysis of thematic maps exhibiting the heterogeneity at a specific scale and resolution (Stein and De Beurs, 2005). They provide a global summary of neighborhood types obtained. The following metrics were calculated: CA (Contiguity Index), PA (Percentage of built-up area), NP (Number of Patches of built up objects), PD (Patch Density), SI (Shape Index of the built up area) and LPI (Largest Patch Index). Definitions and properties are available from Turner et al. (2001). We use a moving window of size 20 m to calculate these metrics.

2.7. Software

We use Definiens' eCognition software to segment the imagery and classify it into a BFP feature dataset. We then use ESRI's ArcGIS to detect the neighborhood typology by spatial prediction and clustering of the BFPs. Validation using travel data is also done using ArcGIS. Fragstats has been used to calculate the spatial metrics, on sample neighborhood types.

3. Results and Validation

3.1. Classification

Results of OBIA are given in Fig. 2. Patterns of elements such as the river, open spaces, bridges and BFPs are visible. Getis – Ord statistic is used for neighborhood characterization in the next stages.

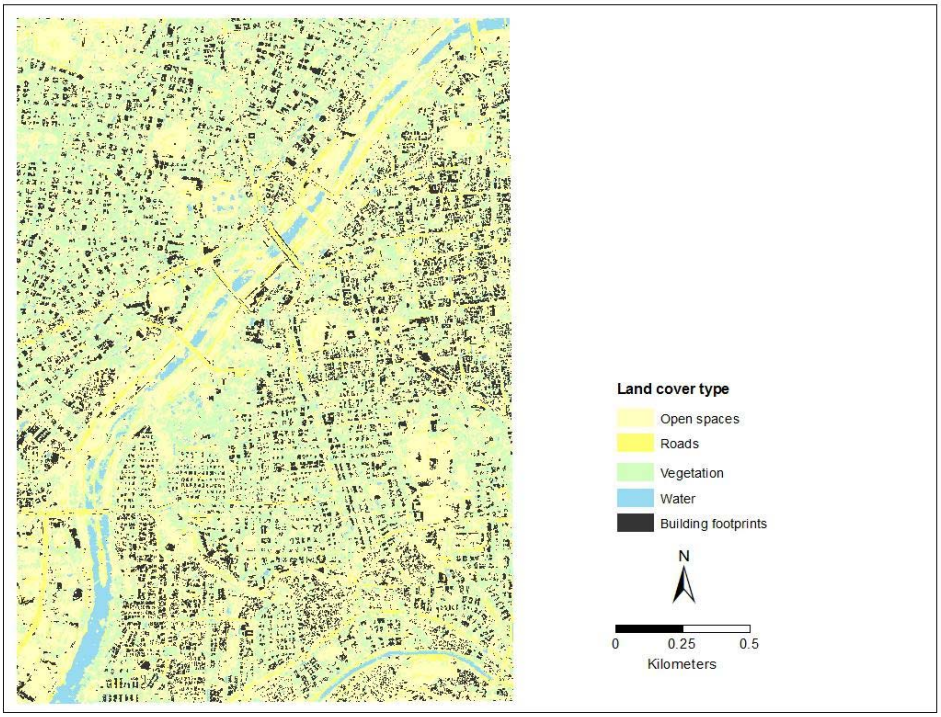

Fig. 2: Classification results from OBIA

3.2. Interpolation

Interpolation of G_i^* values required the construction of a variogram (Fig. 3). A range value of 14.814 m is observed, a value that is again close to 20 m, used during classification. This value corresponds to the average size of buildings in Pune. Observed sill in the variogram equals 9200 DN2and the nugget variance equals 2000 DN2. Hence the spatial component variance equals 7200 DN2, corresponding to a fraction of spatial variation in the total variation i.e, 78%.

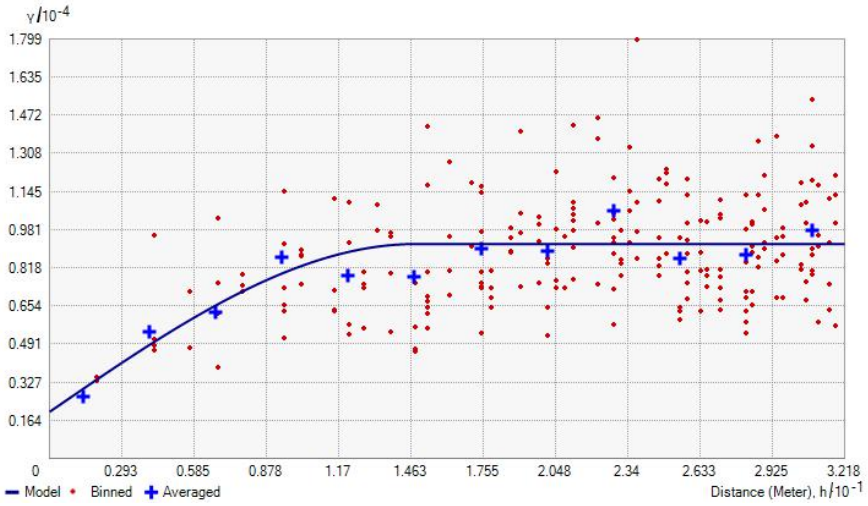

Fig.3: Empirical variogram (dots) and fitted spherical variogram model for red band in the subset. Fitted parameters are c0 = 2000 DN2, c1 = 7200 DN2 and a = 14.814 km.

G_i^*local spatial statistic is applied on the BFP dataset, using area as an associated value (Fig. 4). Calculations resulted in an overall Z-score statistics equal to -22.08, which is highly significant at the 99.99% level. Then, the geostatistical layer is superimposed on the BFPs with the Getis-Ord(G_i^*) Z-score value as an attribute. We chose 19 contour classes for visualizing

the result (Fig.5). Areas of a high and low intensity are found in the map. Thus, we get a first impression of the possibly connected regions, serving as a foundation for the neighborhood structure, we later illustrate.

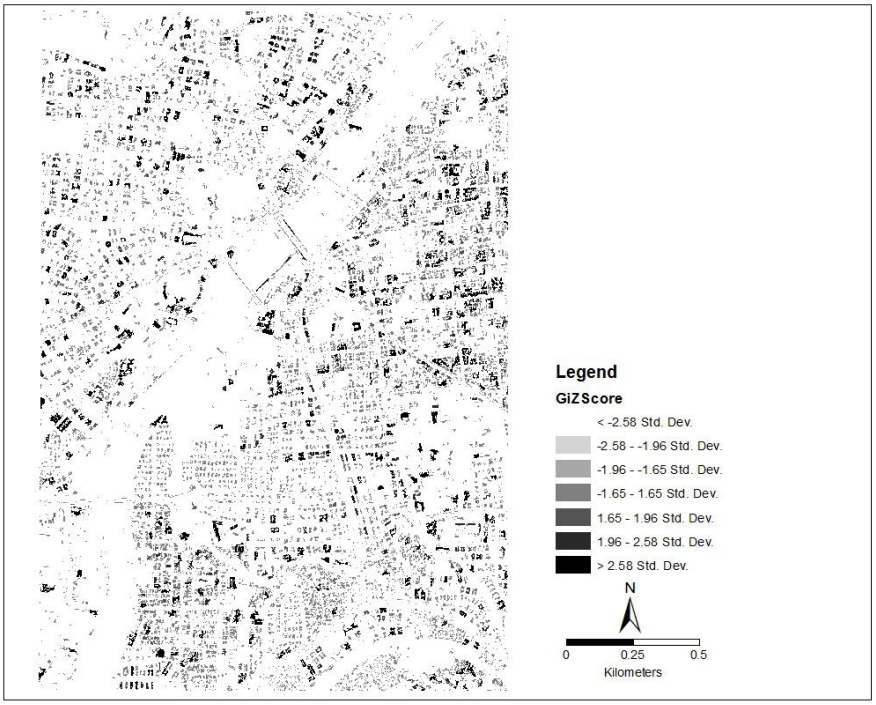

Fig. 4: Z-score value map, derived from the Getis-Ord (G_i^*) local spatial statistics.

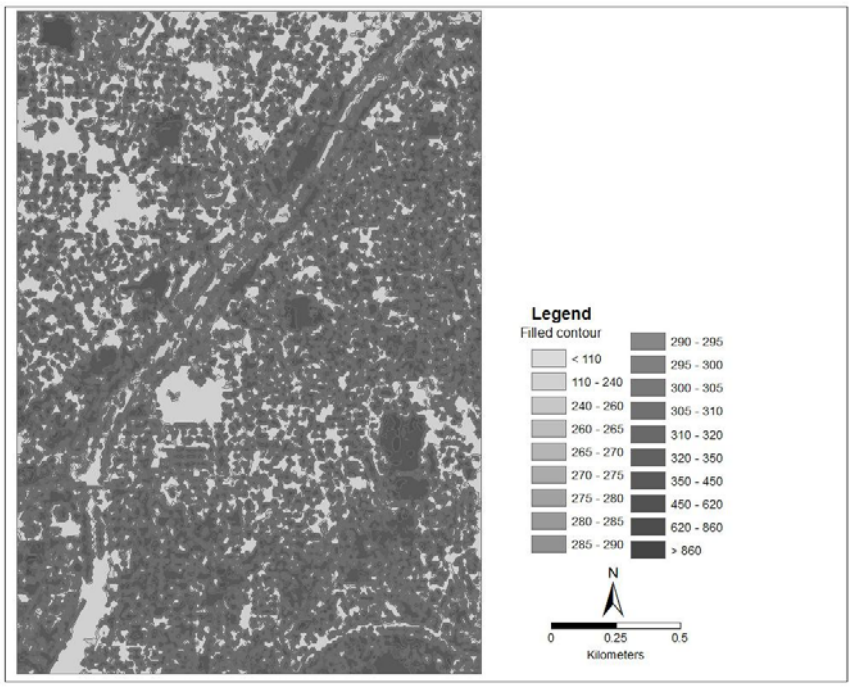

Fig.5: Filled contour map, obtained by ordinary Kriging using the fitted variogram model from Fig. 3

3.3. Integration

Integrating the results of two models is done using the selected threshold contour for each neighborhood boundary. We found the mean value equal to 301.9 from the predicted layer, with a standard deviation equal to 99.8. This value corresponds to the square root of the sill value (95.9). Similar observations are made from the first (228) and third (354) quartile i.e. both values are associated with distinct underlying properties of urban classes.

To obtain the neighborhood dataset, we compare the effects, using 280, 290 and 300 DN contours. 290 DN contour is found useful as a neighborhood boundary. 280 and 290 are discarded, as they show either a number of small, unconnected patches or are randomly located. 300 shows the city as a single neighborhood (figures not shown). Values above 290 are associated with highly clustered BFPs having high positive Z-score values and this explains the results from 300 DN contour. Finally, polygons of urban patches are created above and below 290 DN contour (Fig. 6). Superimposed BFPs

with Z-score are clipped, for the corresponding urban patches. Finally average Z-score values are calculated for each urban patch.

Fig.6: Neighborhood type based on the average Z-score value at filled

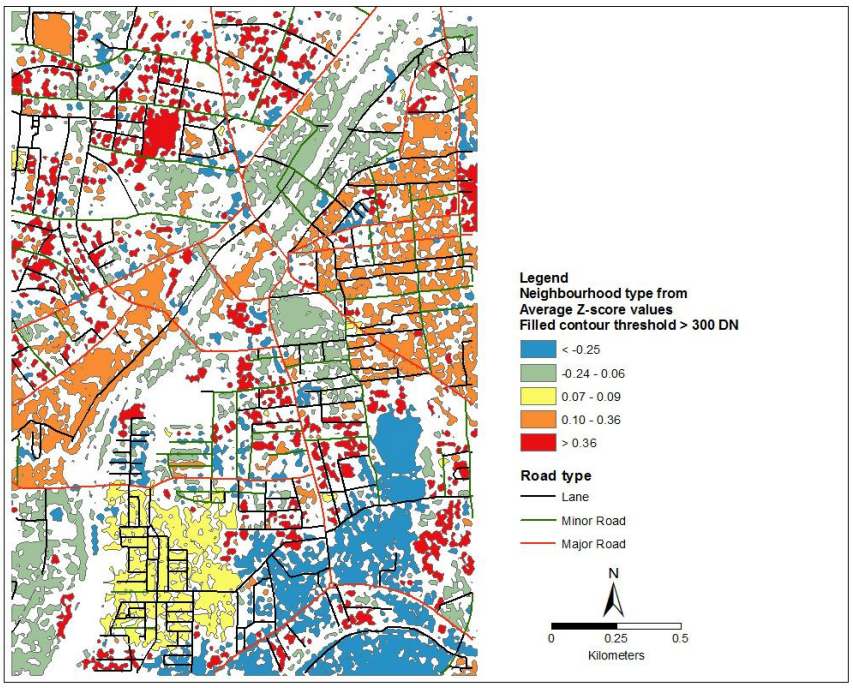

threshold contour >290 DN for each urban patch.

3.4. Neighborhood Types

Based on the results, we identify five types of densities for neighborhood types from the distinct urban patches. Their characteristics explained by the Z-Score are given here:

HCS: Highly clustered, small area. The HCS neighborhood has ($Z < -0.25$). Such a low Z-score shows an area with intensely clustered BFPs, smaller in size. In these neighborhoods the vegetation cover is low. Such neighborhoods are probably exhibiting slum characteristics.

MCS: Moderately clustered, small area. The MCS neighborhood has($-0.24 < Z < -0.06$). They contain clusters of BFPs with small areas but with a less intense clustering pattern than the HCS neighborhoods. BFPs here, exhibit a regular pattern. Vegetation cover is limited.

NCA: Non-clustered, average size. The NCA neighborhood has ($-0.06 < Z < 0.09$). It show a random pattern and are located in the central city. Randomness indicates regularity in clustering of BFPs within these neighborhoods. In addition, we observe a regular pattern of minor roads and lanes within these neighborhoods.

MCL: Moderately clustered pattern of BFPs of a relatively large area has($0.10 < Z < 0.36$) are less intensely clustered and are likely to planned regular developments. They show good vegetation and feature a regular pattern of the minor roads and lanes.

HCL: High clustering pattern of BFPs with larger areas has ($Z > 0.36$) are intensely clustered developments with much larger BFPs. These neighborhoods could contain spaced multilevel structures with significant vegetation. They also feature a regular pattern of the minor roads and lanes. They could either be individual houses or multistoried structures or to the industrial areas.

For each neighborhood type, various class metrics are given in Table 2. We notice that the NCA neighborhood is extreme in various aspects: it has the largest CA value, the largest NP value, the lowest LPI value and the highest LSI value. It is thus clearly clustered, contains many patches, with an average small size and irregular shape. The HCS neighborhood as another extreme has a low CA value, a low NP value, but a high LPI value and a low LSI value. Nly a few patches exhibit a regular structure, which is explained by building clusters packed close, in small areas. HCL neighborhoods remarkably, fall in between NCA and HCS, as exhibited by various metrics. For this neighborhood type, a map of the different metrics is provided in Fig. 7.

Neighborhood Type/ Spatial Metric	CA	PA	NP	PD	LPI	LSI
HCS	1.33	12.99	451	4395	0.77	28.65
MCS	7.53	17.57	1913	4461	0.26	58.26
NCA	13.97	16.15	3200	3700	0.15	74.80
MCL	4.02	10.62	694	1834	0.35	38.21
HCL	6.42	11.02	1429	2452	0.19	49.36
HCS	1.33	12.99	451	4395	0.77	28.65

Table 2: Statistical measures applied on the neighborhoods for validation.

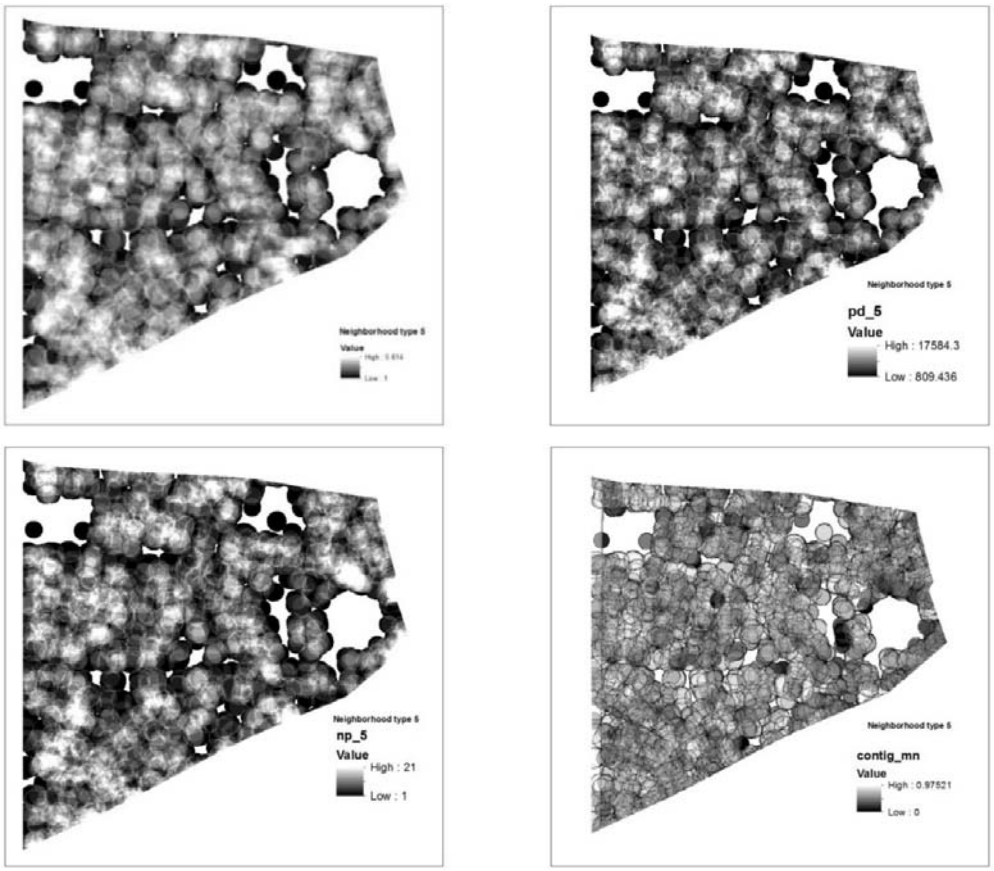

Fig.7: Landscape shape index (LSI), Patch density index (PDI), Number of patches (NP) and Contiguity Index Distribution (CID) for the HCL neighborhood. Similar maps were obtained for the other neighborhood types.

Results of the spatial statistical model, used on the subset so far are then expanded to the entire data of Pune city. Neighborhood typology map is created and individual polygons of each neighborhood type are termed, neighborhood clusters. The map is presented in Fig 8.

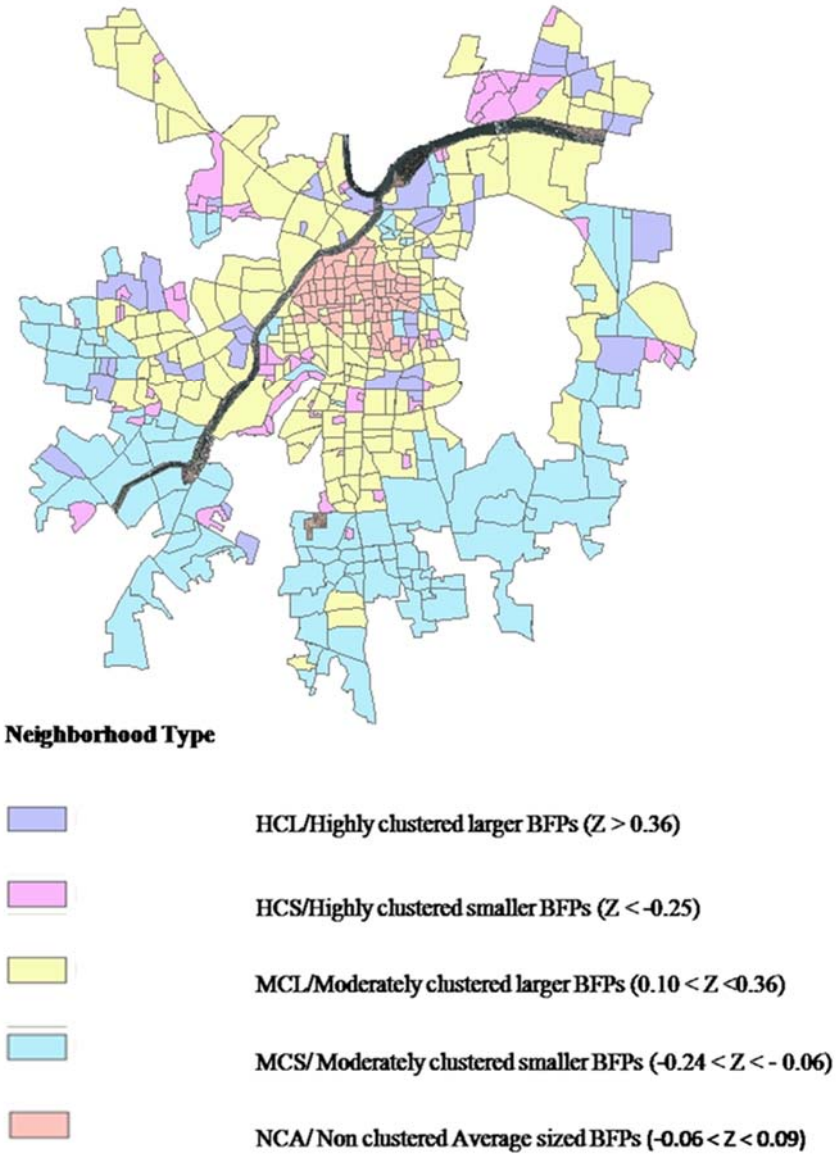

Fig.8: Neighborhood typology, obtained for Pune city, expanding the method citywide, from the subset

3.5. Validation of the Neighborhoods using Travel data

This study uses travel data to validate the types of neighborhoods, obtained from a travel behavior survey conducted in Pune city. Bicycle volume data is integrated with the road network map, collected from a data collection survey of the city office. The bicycle volume map is presented in Fig 9.

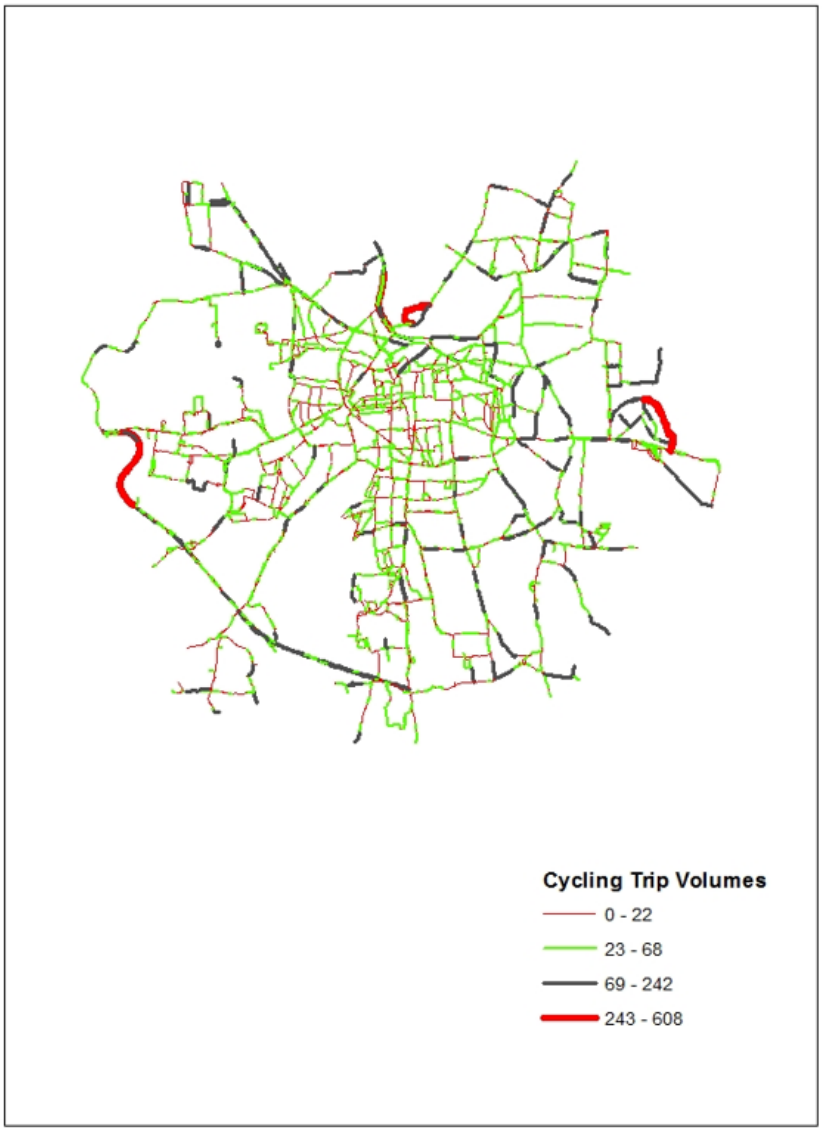

Fig 9: Cycling trip volume data used for validating the neighborhood types obtained from the spatial statistical model

An overlay spatial analysis is conducted, using the Neighborhood type and Bicycle volume datasets. Results present the bicycle volume, corresponding to each neighborhood type (Detailed to each neighborhood cluster, per type). Fig 10 exhibits a scatter plot, exhibiting the results and distinct clusters of bicycle volumes are found per neighborhood type. Table 3shows the results of the spatial overlay analysis.

Neighborhood Category	Neighborhood Cluster Number	Total volume of bicycle trips	Radius (Km)	Percentage of bicycle trips
NSC	NSC1	6440	1.5245	5.3
MCL	MCL1	19200	2.247	15.8
	MCL2	908	1.099	0.7
	MCL3	3118	1.5065	2.6
	MCL4	2627	1.6725	2.2
	MCL5	5033	1.4305	4.1
	MCL6	5083	1.6765	4.2
	MCL7	5950	1.829	4.9
	MCL8	16519	2.241	13.6
MCS	MCS1	11712	2.2585	9.6
	MCS2	12222	2.743	10.1
	MCS3	1897	1.137	1.6
	MCS4	5056	1.45	4.2
	MCS5	7646	2.0175	6.3
HCL	HCL1	1473	0.7965	1.2
	HCL2	414	0.465	0.3
	HCL3	1262	0.548	1.0
HCS	HCS1	3599	1.103	3.0
	HCS2	7301	1.067	6.0
	HCS3	1330	0.637	1.1
	HCS4	2803	0.8245	2.3

Table 3: Bicycle trip volumes per neighborhood type

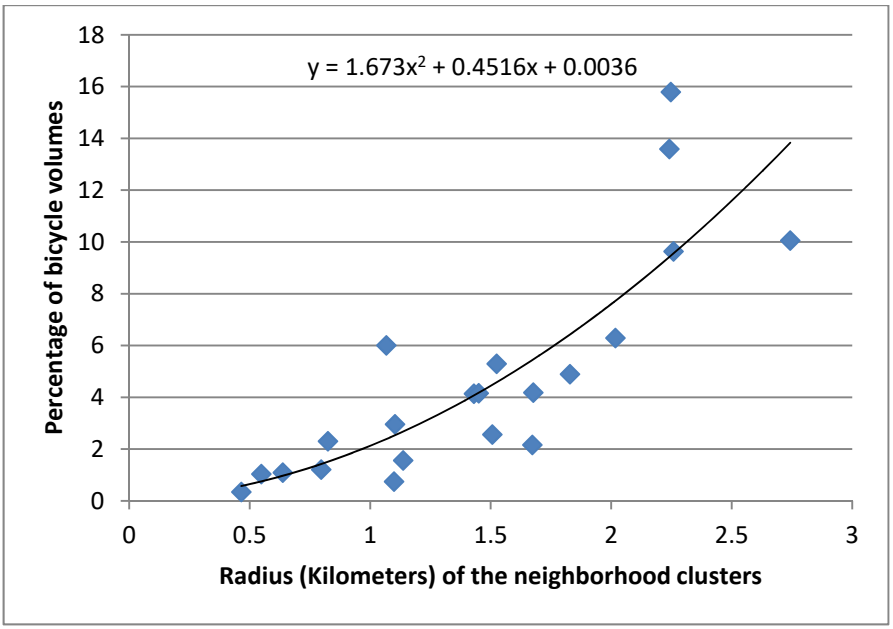

Fig 10: Scatter plot showing the distribution of the bicycle volume data, against the neighborhood types (radius of each neighborhood type is used for X), found in Pune

4. Discussion and Conclusion

We address the spatial characterization of neighborhoods in this study. While directed at identifying clusters of homogenous built up areas, the work also highlights a number of generic challenges typically faced in such studies, when attempted at various scales, and while using different spatial resolutions.

We use a combination of geostatistics and Getis-Ord statistic together with OBIA techniques to achieve the aim of our study. The challenge was to successfully integrate these statistical measures, so that we can use the average Z- score value of the urban patches in interpreting neighborhoods. OBIA overcomes problems of pixel based classification that usually lead to a scattered pattern and are thus, less adequate to derive neighborhoods, by aggregating objects with homogeneity criteria. This aggregation is an essential criterion for transportation planning applications and OBIA bridges the gap, thus. However, there are challenges, in examining the role of spatial scale

and resolution. Effect of the scale parameter on various spatial resolutions when attempting to derive built up objects is a challenging subject that can demand further research.

We conclude that neighborhoods, which can work as units for transportation planning applications are identifiable, by applying spatial statistical models on Quick Bird data. An understanding of the bicycle volume data recorded in the neighborhoods validates the typology, revealing a distinction per neighborhood type. Nevertheless, the research highlights the need to investigate other socio economic indicators, against the neighborhood types. Such investigations could provide spatially meaningful transportation models in the NMT planning context. To this end, the research needs to be tested in other cities dissimilar to Pune, to discern how distinct neighborhood typologies can be, specific to the size and form of each city.

References

Ainsworth, J.W. (2002). Why does it take a village? The mediation of neighborhood effects on educational achievement. Social Forces 81, 117–152.

Atkinson, P. (2002). Spatial Statistics. In A. Stein, F. Meer & B. Gorte (Eds.), Spatial Statistics for Remote Sensing (Vol. 1, pp. 57-81): Springer Netherlands.

Bronfenbrenner, U. (1977). Toward an experimental ecology of human development. American Psychologist 32, 513–531.

Cao, X., Mokhtarian, P. L., Handy, S. L. (2009). The relationship between the built environment and non-work travel: A case study of Northern California. Transportation Research Part A: Policy and Practice, 43(5), 548-559.

Cervero, R., Kockelman, K.M. (1997). Travel demand and the 3Ds: Density, diversity, and design. Transportation Research Part D: Transport and Environment, 2, 199-219.Chen, Y., Shi, P., Fung, T.,

Curran, P. J., Atkinson, P.M. (1998).Geostatistics and remote sensing. Progress in Physical Geography, 22(1), 61-78.

Ebert, A., Kerle, N., Stein, A. (2009) Urban social vulnerability assessment with physical proxies and spatial metrics derived from air- and spaceborne imagery and GIS data. Natural Hazards, 48 (2), pp. 275–294

Ewing, R., Cervero, R. (2010). Travel and the Built Environment.Journal of the American Planning Association, 76, 265-294.

Frank, L., Pivo, G. (1994). Impacts of Mixed use and Density on Utilization of Three Modes of Travel: Single-Occupant Vehicle, Transit and Walking. Transport Research Record, 1466, 44-52

Getis, A. (2010). Spatial Autocorrelation. In M. M. Fischer & A. Getis (Eds.), Handbook of Applied Spatial Analysis (pp. 255-278): Springer Berlin Heidelberg.

Gim, T.H.T. (2012). A meta-analysis of the relationship between density and travel behavior.Transportation, 39, 491-519.Gómez-Hernández, J. (2005).Geostatistics. In Y. Rubin & S. S. Hubbard (Eds.), Hydro geophysics (Vol. 50, pp. 59-83): Springer Netherlands.

Hipp, J. (2010) What is the 'Neighborhood' in Neighborhood Satisfaction? Comparing the Effects of Structural Characteristics Measured at the Micro-neighborhood and Tract Levels. Urban Studies vol. 47, 12: pp. 2517-2536.

Isaaks, E. H., Srivastava, R. M. (1989). An Introduction to Applied Geostatistics: Oxford University Press.

Jupp, D.L.B., Strahler, A.H., Woodcock, C.E. (1988). Autocorrelation and regularization in digital images. I. Basic theory. Geoscience and Remote Sensing, IEEE Transactions on, 26(4), 463-473.

Kwan, M.-P., Weber, J. (2008). Scale and accessibility: Implications for the analysis of land use-travel interaction. Applied Geography, 28(2), 110-123.

LeDrew, E. F., Holden, H., Wulder, M. A., Derksen, C., Newman, C. (2004). A spatial statistical operator applied to multidate satellite imagery for identification of coral reef stress. Remote Sensing of Environment, 91(3-4), 271-279.

Lin, G. (2004). Comparing spatial clustering tests based on rare to common spatial events. Computers, Environment and Urban Systems, 28(6), 691-699.

Morenoff, J.D. (2003). Neighborhood mechanisms and the spatial dynamics of birth weight.American Journal of Sociology 108, 976–1017.

Osgood, D.W., Anderson, A.L. (2004). Unstructured socializing and rates of delinquency. Criminology 42, 519–550.

Park, R.E., Burgess, E.W. (1921). Introduction to the Science of Sociology.University of Chicago, Chicago.

Ross, C.E., Reynolds, J.R., Geis, K.J. (2000). The contingent meaning of neighborhood stability for residents' psychological well-being. American Sociological Review 65, 581–595

Schwanen, T., Mokhtarian, P. L. (2005). What if you live in the wrong neighborhood? The impact of residential neighborhood type dissonance on distance traveled. Transportation Research Part D: Transport and Environment, 10(2), 127-151.

Schwarz, N. (2010). Urban form revisited - Selecting indicators for characterizing European cities. Landscape and Urban Planning, 96(1), 29-47.

Shaw, C., McKay, H.D., 1942. Juvenile Delinquency and Urban Areas. University of Chicago Press, Chicago.

Silver, E., Miller, L.L., 2004.Sources of informal social control in Chicago neighborhoods. Criminology 42, 551–584.

Sliuzas, R. V., Kerle, N., Kuffer, M. (2008).Object-oriented mapping of urban poverty and deprivation. In Paper presented at the EARSeL workshop on remote sensing for developing countries in conjunction with GISDECO 8, Istanbul, Turkey.

Song, Y., Knaap, G.J. (2007). Quantitative Classification of Neighborhoods: The Neighborhoods of New Single-family Homes in the Portland Metropolitan Area. Journal of Urban Design, 12(1), 1-24.

Stead, D., Marshall, S. (2001). The relationships between urban form and travel patterns: an international review and evaluation. European Journal of Transport and Infrastructure Research, 1(2), 113-141.

Stein, A., De Beurs, K. (2005). Complexity metrics to quantify semantic accuracy in segmented Landsat images .International Journal of Remote Sensing 26 (14), 2937 – 2951.

Tang, J., Wang, L., & Yao, Z. (2008). Analyses of urban landscape dynamics using multi-temporal satellite images: A comparison of two petroleum-oriented cities. Landscape and Urban Planning, 87(4), 269-278.

Turner, M.G., Gardner, R.H., O'Neill, R.V. (2001). Landscape ecology in theory and practice: pattern and process. Dordrecht, Kluwer.

Yoshida, H., Omae, M. (2005). An approach for analysis of urban morphology: methods to derive morphological properties of city blocks by using an urban landscape model and their interpretations. Computers, Environment and Urban Systems, 29(2), 223-247.